



Bowman, R., Jesacher, A., Thalhammer, G., Gibson, G., Ritsch-Marte, M., and Padgett, M. (2011) *Position clamping in a holographic counterpropagating optical trap*. *Optics Express*, 19 (10). pp. 9908-9914. ISSN 1094-4087 (doi:10.1364/OE.19.009908)

<http://eprints.gla.ac.uk/59790/>

Deposited on: 11th September 2012

Position clamping in a holographic counterpropagating optical trap

Richard Bowman,^{1,*} Alexander Jesacher,² Gregor Thalhammer,²
Graham Gibson,¹ Monika Ritsch-Marte,² and Miles Padgett¹

¹Department of Physics and Astronomy, SUPA, University of Glasgow, G12 8QQ, UK

²Division for Biomedical Physics, Innsbruck Medical University, Müllerstr. 44, A-6020, Innsbruck, Austria

<http://www.physics.gla.ac.uk/optics>

*r.bowman@physics.gla.ac.uk

Abstract: Optical traps consisting of two counterpropagating, divergent beams of light allow relatively high forces to be exerted along the optical axis by turning off one beam, however the axial stiffness of the trap is generally low due to the lower numerical apertures typically used. Using a high speed spatial light modulator and CMOS camera, we demonstrate 3D servocontrol of a trapped particle, increasing the stiffness from 0.004 to $1.5 \mu\text{Nm}^{-1}$. This is achieved in the “macro-tweezers” geometry [Thalhammer, *J. Opt.* **13**, 044024 (2011); Pitzek, *Opt. Express* **17**, 19414 (2009)], which has a much larger field of view and working distance than single-beam tweezers due to its lower numerical aperture requirements. Using a $10\times$, 0.2NA objective, active feedback produces a trap with similar effective stiffness to a conventional single-beam gradient trap, of order $1 \mu\text{Nm}^{-1}$ in 3D. Our control loop has a round-trip latency of 10ms, leading to a resonance at 20Hz. This is sufficient bandwidth to reduce the position fluctuations of a $10 \mu\text{m}$ bead due to Brownian motion by two orders of magnitude. This approach can be trivially extended to multiple particles, and we show three simultaneously position-clamped beads.

© 2011 Optical Society of America

OCIS codes: (140.7010) Laser trapping; (230.6120) Spatial light modulators; (120.4640) Optical instruments; (350.4855) Optical tweezers or optical manipulation.

References and links

1. S. B. G. Thalhammer, R. Steiger, and M. Ritsch-Marte, “Optical macro-tweezers: trapping of highly motile micro-organisms,” *J. Opt.* **13**(4), 044024 (2011).
2. M. Pitzek, R. Steiger, G. Thalhammer, S. Bernet, and M. Ritsch-Marte, “Optical mirror trap with a large field of view,” *Opt. Express* **17**(22), 19414–19423 (2009).
3. A. Ashkin, J. M. Dziedzic, J. E. Bjorkholm, and S. Chu, “Observation of a single-beam gradient force optical trap for dielectric particles,” *Opt. Lett.* **11**(5), 288–290 (1986).
4. K. Svoboda, C. Schmidt, B. Schnapp, and S. M. Block, “Direct observation of Kinesin stepping by optical trapping interferometry,” *Nature* **365**(6448), 721–727 (1993).
5. J. Molloy and M. Padgett, “Lights, action: optical tweezers,” *Contemp. Phys.* **43**(4), 241–258 (2002).
6. K. Neuman and S. M. Block, “Optical trapping,” *Rev. Sci. Instrum.* **75**(9), 2787–2809 (2004).
7. M. Reicherter, T. Haist, E. Wagemann, and H. Tiziani, “Optical particle trapping with computer-generated holograms written on a liquid-crystal display,” *Opt. Lett.* **24**(9), 608–610 (1999).
8. D. G. Grier, “A revolution in optical manipulation,” *Nature* **424**(6950), 810–816 (2003).

9. G. Sinclair, P. Jordan, J. Leach, M. Padgett, and J. Cooper, "Defining the trapping limits of holographical optical tweezers," *J. Mod. Opt.* **51**(3), 409–414 (2004).
10. A. Ashkin, "Acceleration and trapping of particles by radiation pressure," *Phys. Rev. Lett.* **24**(4), 156–159 (1970).
11. P. Rodrigo, V. Daria, and J. Glückstad, "Four-dimensional optical manipulation of colloidal particles," *Appl. Phys. Lett.* **86**(7), 074103 (2005).
12. P. J. Rodrigo, L. Kelemen, D. Palima, C. A. Alonzo, P. Ormos, and J. Glückstad, "Optical microassembly platform for constructing reconfigurable microenvironments for biomedical studies," *Opt. Express* **17**(8), 6578–6583 (2009).
13. A. Constable, J. Kim, J. Mervis, F. Zarinetchi, and M. Prentiss, "Demonstration of a fiberoptic light-force trap," *Opt. Lett.* **18**(21), 1867–1869 (1993).
14. J. Guck, R. Ananthakrishnan, H. Mahmood, T. J. Moon, C. C. Cunningham, and J. Käs, "The optical stretcher: a novel laser tool to micromanipulate cells," *Biophys. J.* **81**(2), 767–784 (2001).
15. S. Zwick, T. Haist, Y. Miyamoto, L. He, M. Warber, A. Hermerschmidt, and W. Osten, "Holographic twin traps," *J. Opt. A* **11**(3), 034011 (2009).
16. M. Woerdemann, K. Berghoff, and C. Denz, "Dynamic multiple-beam counter-propagating optical traps using optical phase-conjugation," *Opt. Express* **18**(21), 22348–22357 (2010).
17. I. Perch-Nielsen, P. Rodrigo, and J. Glückstad, "Real-time interactive 3D manipulation of particles viewed in two orthogonal observation planes," *Opt. Express* **13**(8), 2852–2857 (2005).
18. S. Tauro, A. Bañas, D. Palima, and J. Glückstad, "Dynamic axial stabilization of counter-propagating beam-traps with feedback control," *Opt. Express* **18**(17), 18217–18222 (2010).
19. K. D. Wulff, D. G. Cole, and R. L. Clark, "Servo control of an optical trap," *Appl. Opt.* **46**(22), 4923–4931 (2007).
20. A. E. Wallin, H. Ojala, E. Haeggstrom, and R. Tuma, "Stiffer optical tweezers through real-time feedback control," *Appl. Phys. Lett.* **92**(22), 224104 (2008).
21. J. E. Molloy, J. E. Burns, J. Kendrick-jones, R. T. Tregear, and D. C. S. White, "Movement and force produced by a single myosin head," *Nature* **378**(6553), 209–212 (1995).
22. H. Sehgal, T. Aggarwal, and M. V. Salapaka, "High bandwidth force estimation for optical tweezers," *Appl. Phys. Lett.* **94**(15), 153114 (2009).
23. R. W. Bowman, G. Gibson, and M. Padgett, "Particle tracking stereomicroscopy in optical tweezers: control of trap shape," *Opt. Express* **18**(11), 11785–11790 (2010).
24. D. Preece, R. W. Bowman, A. Linnenberger, G. Gibson, S. Serati, and M. Padgett, "Increasing trap stiffness with position clamping in holographic optical tweezers," *Opt. Express* **17**(25), 22718–22725 (2009).
25. R. W. Bowman, D. Preece, G. Gibson, and M. J. Padgett, "Stereoscopic particle tracking for 3D touch, vision and closed-loop control in optical tweezers," *J. Opt. A* **13**(4), 044003 (2011).
26. O. Otto, F. Czerwinski, J. L. Gornall, G. Stober, L. B. Oddershede, R. Seidel, and U. F. Keyser, "Real-time particle tracking at 10,000 fps using optical fiber illumination," *Opt. Express* **18**(22), 22722–22733 (2010).
27. S. A. Alexandrov, T. R. Hillman, T. Gutzler, and D. D. Sampson, "Synthetic aperture fourier holographic optical microscopy," *Phys. Rev. Lett.* **97**(16), 168102 (2006).
28. S.-H. Lee and D. G. Grier, "Holographic microscopy of holographically trapped three-dimensional structures," *Opt. Express* **15**(4), 1505–1512 (2007).
29. J. S. Dam, I. R. Perch-Nielsen, D. Palima, and J. Glückstad, "Three-dimensional imaging in three-dimensional optical multi-beam micromanipulation," *Opt. Express* **16**(10), 7244–7250 (2008).
30. J. S. Dam, I. Perch-Nielsen, D. Palima, and J. Glückstad, "Multi-particle three-dimensional coordinate estimation in real-time optical manipulation," *J. Eur. Opt. Soc. Rapid Publ.* **4**, 09045 (2009).

1. Introduction

Optical tweezers [3] has now become a standard technique for trapping, manipulation and force measurement [4, 5] in micron-sized physical and biological systems [6]. This has been extended by the use of Spatial Light Modulators (SLMs) to allow multiple particles to be manipulated interactively in three dimensions [7, 8] over a range of order $100\ \mu\text{m}$ [9]. In its usual form, a holographic optical tweezer system uses a high-NA microscope objective to generate an intensity maximum which is tightly localised in three dimensions to give axial trapping due to the gradient force which can overcome the scattering force. However, two counterpropagating, diverging beams can also trap particles [10], using opposing objective lenses [11, 12], fibres [13, 14], a mirror behind the sample [2, 15] or even optical phase conjugation [16]. In this configuration the scattering forces from the two beams cancel out when the particle is in the centre, and act to push the particle back when it is displaced axially. This removes the requirement for high numerical aperture, and enables the use of long working distance objectives and lower

magnifications than are typically used for single beam tweezers.

The use of lower magnification objectives also opens up the possibility of manipulating larger objects [1] and of adding a side view to the system [17]. Both of these can use multiple objective lenses [10, 18], however it is also possible to use a single objective with a modified sample cell. By placing a mirror behind the sample, it is possible to use a holographic system to create foci in front of and behind the mirror [2, 15], referred to as “macro-tweezers” [1]. The mirror then reflects one of these foci to create two foci with opposite directions of propagation, as shown in Fig. 1. By adding a prism at the side, we can use the same objective to view the sample from two orthogonal directions [1].

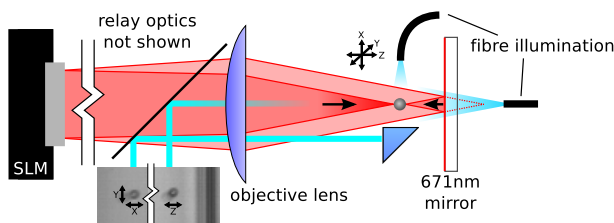


Fig. 1. Schematic of the trapping and imaging system. The laser is split into two beams with the SLM, one of which is reflected by the mirror to form a backward-propagating focus. A prism provides a side view, from which we can find the axial position of objects.

Counterpropagating traps can achieve very high axial forces by turning off the upwards- or downwards-propagating beam. However, the axial stiffness is usually very low, meaning that Brownian motion causes the particle’s axial position to vary by as much as several microns, complicating accurate positioning or force measurement in the axial direction. This combination of low stiffness and high maximum force makes the system an ideal candidate for closed loop control. In this article, we describe the implementation of feedback control in macro-tweezers, using a fast SLM and CMOS camera. The use of these technologies allows us to attain a bandwidth an order of magnitude higher than that previously reported using a GPC-based system [18], resulting in much smaller residual motion and a greatly reduced resonance.

Position clamping in single-beam gradient traps [19, 20, 21, 22] requires a bandwidth of many kHz to achieve a large suppression of residual Brownian motion. However, the larger objects which can be trapped in counterpropagating traps exhibit less high-frequency motion due to the greater viscous drag forces they experience. This means that a lower bandwidth is required in the servo loop, making it more easily accessible with cameras and SLMs.

2. Method

2.1. Optical System

Figure 2 shows our optical system, similar to that described in [23] but with an Olympus 10x, 0.2NA objective, and a different focal length lens in front of the SLM to fill the objective’s back aperture. A 300mW, 671 nm DPSS laser system (Roithner LaserTechnik) was used, and a corresponding band-reflecting mirror was placed behind the sample. Two fibres, similar to those in [23], were used to illuminate the sample from above and from the side. The sample cell was prepared as in [2], with a square cross-sectioned cuvette (VitroCells 8240) and a miniature right-angle prism (NT45-385, Edmund Optics). An air gap underneath the cell ensures the focal planes for the bottom and side views coincide approximately in the middle of the cell.

The fast SLM (Boulder Nonlinear Systems) runs at 203Hz, controlled by our low-latency OpenGL software [24] to minimise delays in the control loop. A fast CMOS camera (Mikrotron EoSens 1362-CL) was used to monitor the position of the bead from the two viewpoints which

allowed recovery of its 3D position. Image acquisition and control logic were performed in LabVIEW (National Instruments). Regions were defined on the camera corresponding to bottom and side views, then smaller regions were extracted around the trapped particles, which were tracked with a symmetry transform implemented in C [25]. A CameraLink Full framegrabber (National Instruments PCIe 1433) provided sufficient bandwidth to run the camera at 1 kHz with a field of view 1280×512 pixels (1.6×0.6 mm) across.

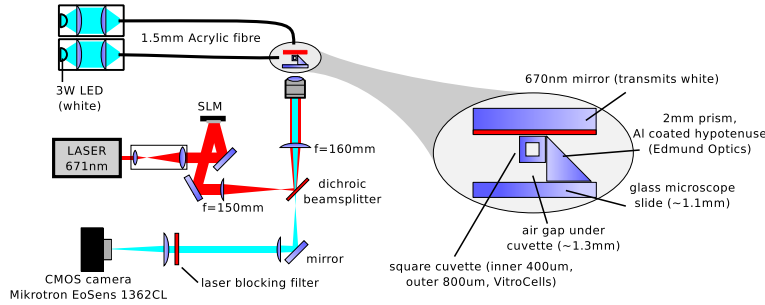


Fig. 2. Sample cell and optical system used in the experiment.

2.2. Control Logic

Trapped objects can be moved in z either by axially shifting the two foci or by adjusting the balance of power between the upper and lower beams, keeping total power constant. The latter method allows large forces to be exerted, so we use this to effect closed-loop control. Shifting the foci allows the bead to be moved over a large axial range while keeping the foci relatively close (thus maximising the lateral force), so we use this to position the bead in open-loop mode. The foci are centred on the position set-point in closed loop mode. Changing intensities can also change the equilibrium position with fixed focal planes [18], however stable traps can only be formed between the two foci, limiting either the axial range or the maximum lateral force.

To minimise the displacement of the bead from the setpoint, we use a simple proportional controller [20, 24] i.e. the balance of power in the two beams $\beta = (P_{\text{up}} - P_{\text{dn}})/P_{\text{total}} = a_z \Delta z$ where Δz is displacement, a_z is feedback gain and P_{up} , P_{dn} are the powers in the two beams. However, as the force due to changing β is nearly independent of the particle's position, the controller is effectively integrated by the bead on timescales smaller than the autocorrelation time, which is several seconds ($\dot{z}_{\text{bead}} \propto \beta$ and hence $z_{\text{bead}} \propto \int \beta$).

The control loop runs at 1 kHz, the speed of the camera. The SLM is updated each time it refreshes, which occurs at the maximum frame rate (203Hz). Our round trip latency is in the region of 10ms, which means the servo loop becomes resonant at around 20Hz. This is a significant limitation when working with small objects where there is significant Brownian motion above this frequency, which cannot be compensated for with servocontrol. However, the larger objects which can be trapped in counterpropagating traps are more strongly damped by the surrounding fluid, and consequently they exhibit less high-frequency motion. This means that more of their Brownian motion can be cancelled out.

3. Results

Using the system described above, a $10 \mu\text{m}$ Silica sphere was held in a trap, and then servo-control was activated laterally, axially, and in 3D. A scatterplot of the bead's motion in y and z is shown in Fig. 3(a). Stiffness in x , y and z (as estimated using the equipartition formula, $\kappa_z = k_B T / \langle z^2 \rangle$) was increased from $(0.14, 0.08, 0.004) \mu\text{Nm}^{-1}$ to $(1.9, 0.85, 1.3) \mu\text{Nm}^{-1}$. A

stiffness of $1.5 \mu\text{Nm}^{-1}$ was reached when the particle was clamped only in z . As the feedback gain is increased, the particle's position fluctuations decrease. Power spectra for axial motion are given in Fig. 3 as a function of gain, along with a plot of effective stiffness against gain. The y axis is the long axis of the cuvette. The ends were closed with valves, but residual fluid flow made the y direction more susceptible to mechanical interference. This, combined with slight misalignments, may explain the lower stiffness in y .

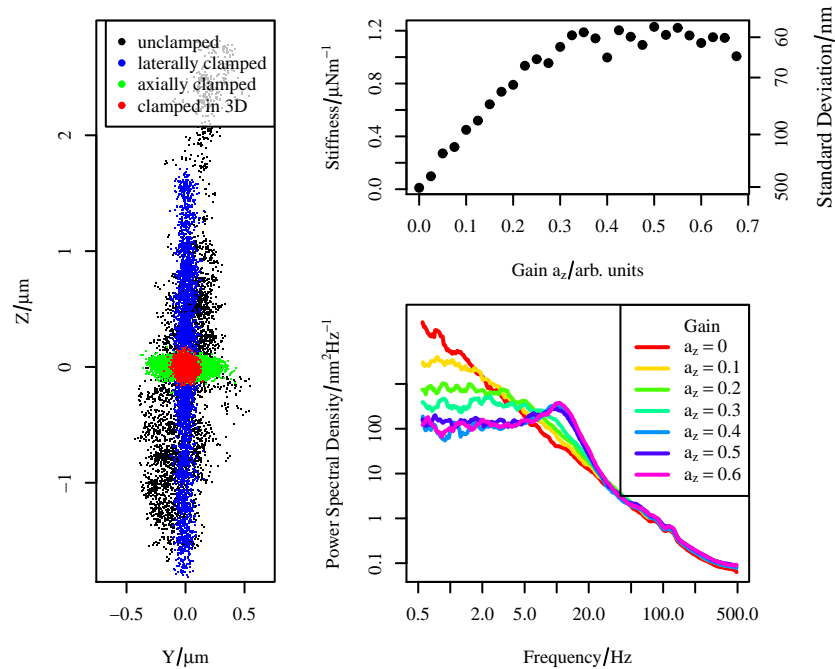


Fig. 3. Scatterplot of the motion of a $10 \mu\text{m}$ Silica particle in the trap with and without feedback (100s of data at 1kHz), along with power spectra of the particle's motion and corresponding stiffness values for different feedback gains a_z in the axial direction.

Active feedback not only reduces position fluctuations, it also improves the speed and settling time when moving particles over longer distances. Fig. 4 shows particle tracks for a $10 \mu\text{m}$ bead moved in a square wave pattern in the axial direction. In open-loop mode, the axial position of the two foci (separated by $20 \mu\text{m}$, chosen to maximise axial stiffness) were shifted to move the trap centre to the position set-point. The axial stiffness is very low, so the relaxation time of the trap was much longer than the few seconds between flips. With closed-loop control, the bead quickly reached the set-point. The response time of the bead was limited by the maximum speed which could be reached by the particle, with all the power in one beam. This is why the response is predominantly linear rather than exponential. The amplitude of $20 \mu\text{m}$ was chosen to prevent the bead being lost from the trap in open-loop mode.

Holographic optical tweezers and camera-based position sensing make it simple to extend closed-loop control to multiple particles: Fig. 4 shows three beads position-clamped in 3D. The stiffness of these traps was approximately $0.7 \pm 0.2 \mu\text{Nm}^{-1}$ in 3D, due at least in part to the laser power being divided between three traps. Provided the regions of interest corresponding to each trap were distinct (i.e. separation $\geq 20 \mu\text{m}$), crosstalk between traps was not observed.

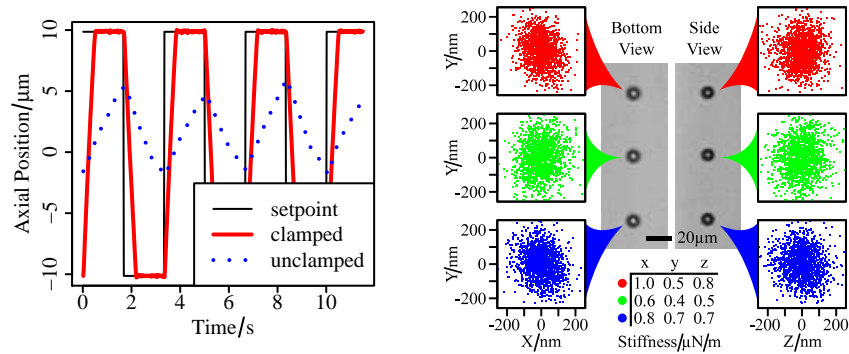


Fig. 4. (left) Response of a $10\mu\text{m}$ bead to a square-wave control signal, with and without feedback (Media 1). (right) Three $10\mu\text{m}$ beads simultaneously clamped in 3D, with scatterplots of their position. Stiffness values are shown below the image.

4. Discussion

The use of closed loop control in a counterpropagating optical trap can significantly increase both the effective stiffness of the trap and the maximum axial force it can apply. The servo-controlled trap is stiff and stable when the two foci are close together, which maximises the available lateral force (in the open loop system one must compromise between axial stability when the foci are well separated and maximum lateral force when they are close together). This is important when manipulating particles over the comparatively large distances, and hence high speeds, accessible using a low-magnification objective. Our implementation uses a high-speed camera [26] and a fast SLM with optimised hologram generation to increase the bandwidth of our system by an order of magnitude compared to the previous work [18]. Also, the ability to axially reposition the foci increases the maximum force available to us compared to a fixed-focal-plane system.

Having a side view allows very simple 3D tracking of particles for closed loop control, and is a useful addition to the existing techniques. Digital holographic microscopy can track objects in 3D [27, 28], but requires demanding image processing making it too slow for closed-loop control at present. It also requires coherent light and often a high-NA objective. Similarly, stereoscopic particle tracking [29, 23, 30, 25] achieves high resolution only in conjunction with high-NA optics. Looking from the side has been implemented using an additional objective [17], however the convenience of a modified sample cell [1] is a significant advantage.

5. Conclusion

We have demonstrated closed loop control of a bead held in a counterpropagating optical trap, generated using a single objective and an SLM. The system has a high enough bandwidth to increase the axial trap stiffness by a factor of 300, thereby suppressing a significant portion of the particle's position fluctuations due to Brownian motion and external disturbances. Closed loop control also provides a stiff trap when the foci are close together axially, which increases the maximum force available laterally as well as axially. This enables faster manipulation of particles in the large workspace available with a low magnification objective, and makes the stiffness of such a trap comparable to a single-beam gradient trap.

Acknowledgements

MRM acknowledges support from the ERC Advanced Grant P 24724 catchIT and MJP acknowledges support from the Royal Society and EPSRC.